17th World Conference on Earthquake Engineering, 17WCEE
Sendai, Japan - September 13th to 18th 2020

SEISMIC UPGRADING BY INSTALLING WING WALLS FOR RC BUILDINGS WITH DEFICIENT BEAM REBAR ANCHORAGE

M. Ahmed [1], S. Wardi [2], Y. Sanada [3], S. Takahashi [4]

[1] *Graduate Student, Graduate School of Engineering, Osaka University, Japan, murshalin_ahmed@arch.eng.osaka-u.ac.jp*
[2] *Lecturer, Department of Civil Engineering, Padang Institute of Technology, Indonesia, wardi.syafri@gmail.com*
[3] *Professor, Graduate School of Engineering, Osaka University, Japan, sanada@arch.eng.osaka-u.ac.jp*
[4] *Associate Professor, Faculty of Engineering, Daido University, Japan, susumu-t@daido-it.ac.jp*

Abstract

Severe damage on reinforced concrete (RC) buildings observed in several earthquakes in developing countries was often caused by the existence of beam-column joints with deficient detailing. This study focuses on the application of RC wing walls for strengthening exterior beam-column joints with deficient beam rebar anchorage and its effectiveness to upgrade the seismic performance of buildings with the above weakness.

First, an experimental study was conducted to investigate the applicability of the strengthening method by installing wing walls on an exterior RC beam-column joint with deficient anchorage of beam longitudinal rebar, which was expected to fail in anchorage. Two 70%-scaled beam-column joint specimens representing a typical Bangladeshi building, one benchmark specimen (J1) and one strengthened specimen by installing wing walls (J1-W), were prepared and tested. The length of wing walls is proposed to extend the development length of beam longitudinal rebar. Experimental results showed that the proposed strengthening method successfully changed the failure mode from brittle anchorage failure (J1) to ductile beam-yielding (J1-W) and increased the strength and ductility of the strengthened specimen (J1-W).

Second, an analytical evaluation was conducted to investigate the effects of the strengthening method on the global seismic performance of the RC building. Pushover analysis was conducted for two models, one model of frame without wing walls and one model of frame with wing walls. The wing walls were installed on the interior side of the exterior columns for all stories of the model building, which was the focused building in the experimental study. Performance limit of the frame without wing walls was assumed as a drift ratio when the strength degradation started due to anchorage failure in specimen J1. On the other hand, the performance limit of the frame with wing walls was determined analytically as a drift ratio when one of the beams initially showed a flexural-shear failure defined as an intersection point of the flexural performance curve and the degraded shear capacity curve of the beam. The analytical results showed that the installation of wing walls increased the strength and the deformation capacity of the building.

This study confirmed that the installation of wing walls was not only effective to strengthen the exterior RC beam-column joints with deficient beam rebar anchorage but also effective to upgrade the global seismic performance of the buildings with deficient beam-column joints.

Keywords: deficient beam rebar anchorage; reinforced concrete building; seismic strengthening; developing country

1. Introduction

Recent earthquakes in developing countries have caused severe damages to the reinforced concrete (RC) buildings. Being the weakest link in the modern RC frame style structure, the beam-column joint comprising of inadequate seismic detailing is highly susceptible to severe damage during seismic events. Many of the existing buildings in Bangladesh do not meet the minimum design requirements, particularly in the sector of beam-column joint detailing, specified in Bangladesh National Building code (BNBC) [1]. The situation got worse once deformed bars were introduced to the local market in 1995. Compared to the plain bar, the development length requirement of the deformed bar is smaller and less strict [1].

In this study, RC wing walls were installed to strengthen exterior joints with deficient beam rebar anchorage. The length of wing walls was set such that it extends the development length of the beam longitudinal rebar to the minimum requirement as defined in building code, which was proposed and verified in the authors' previous study [2]. The present paper summarizes the preceded experimental study and analytically discusses the effects of the above strengthening method by RC wing walls on the global seismic performance of RC buildings with deficient beam rebar anchorage. To evaluate the global seismic performance of the structure, pushover analysis was performed for the building of interest focused on the previous study [2] considering with and without wing walls. The performance limit of the structure was determined by the initiation point of the degradation of structural integrity. For frame without wing walls, it was assumed as the drift ratio when strength degradation started due to anchorage failure. Whereas, for frame with wing walls, the performance limit was analytically evaluated to the point when one of the beams initially showed a flexural-shear failure, which was defined as an intersection point of the flexural performance curve and the degraded shear capacity curve of the beam. Thus, the global seismic performance was compared between the building before and after strengthening by the proposed method.

Lack of proper seismic detailing is widely observed in many developing countries around the world. As a result, the outcome of this study can be used in other developing countries.

2. Experimental Study on Strengthening of Beam-Column Joint with Deficient Beam Rebar Anchorage by Wing Walls

The details of the experimental study were described in the previous study [2]. This section describes the summary of the study briefly.

2.1 Building of interest and specimen details

The exterior beam-column joint of an intermediate story of an RC building was focused in this study. The subject building was an existing six-story RC building in Dhaka city, capital of Bangladesh, as shown in Fig. 1. Low strength concrete incorporating brick chips was used in the construction of test specimens to represent the existing Bangladeshi buildings. The design strength of the concrete was 10 MPa and reinforcement was 295 MPa.

Two 70% scaled specimens were constructed for this experiment: Benchmark specimen J1 and strengthened specimen J1-W. The specimen J1 incorporated deformed bar and straight anchorage for beam longitudinal bars, as shown in Fig. 2(a). The specimen was modeled up to the inflection points of the upper/lower column and beam.

The strengthening method by installing wing walls was proposed to prevent the anticipated failure at exterior beam-column joints [3], in particular, the anchorage failure of beam longitudinal rebar in the present study [2]. The strengthened specimen J1-W was the other specimen representing J1, however, with wing walls installed on the interior side of the column, as shown in Fig. 2(b).

The proposal of consideration of l_w (length of wing walls) for the embedment length of beam longitudinal rebar is not accepted in the Japanese standard [4]; thus, it was verified through the tests. The details of wing walls were designed according to the provisions describing wing walls for the strengthening of the column in

the Japanese guidelines for seismic retrofit of RC buildings [5]. The length of the wing walls was determined by Eq. (1) as per the previous study [2].

$$l_w \geq l_d - {}_{ex}l_d \tag{1}$$

where l_w = length of wing wall; ${}_{ex}l_d$ = existing development length; l_d = required development length.

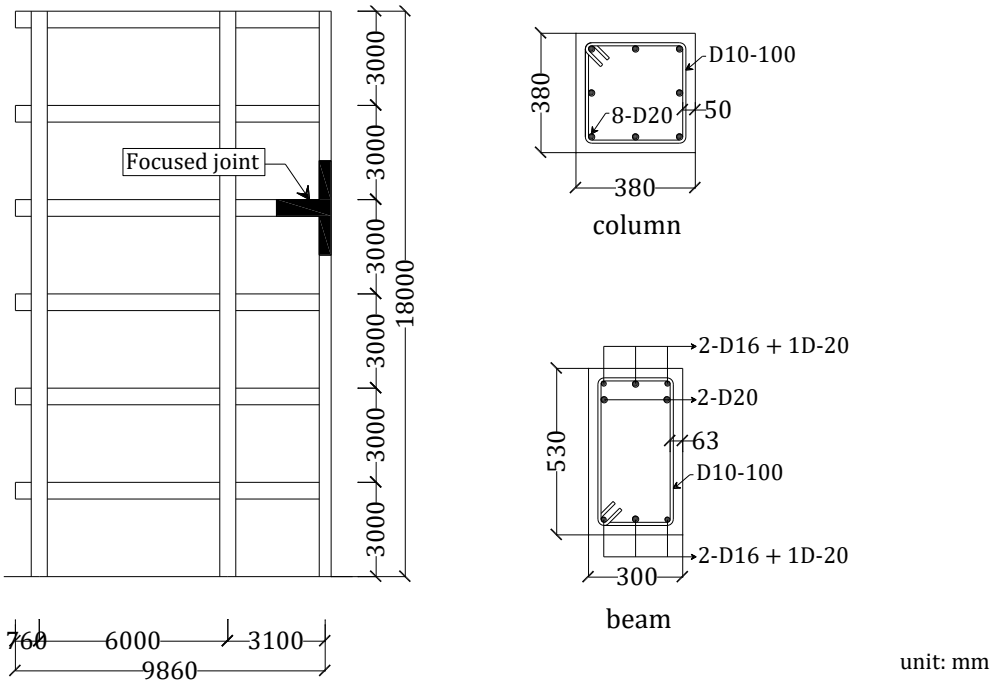

Fig. 1 – Subject building and detail of structural members [2]

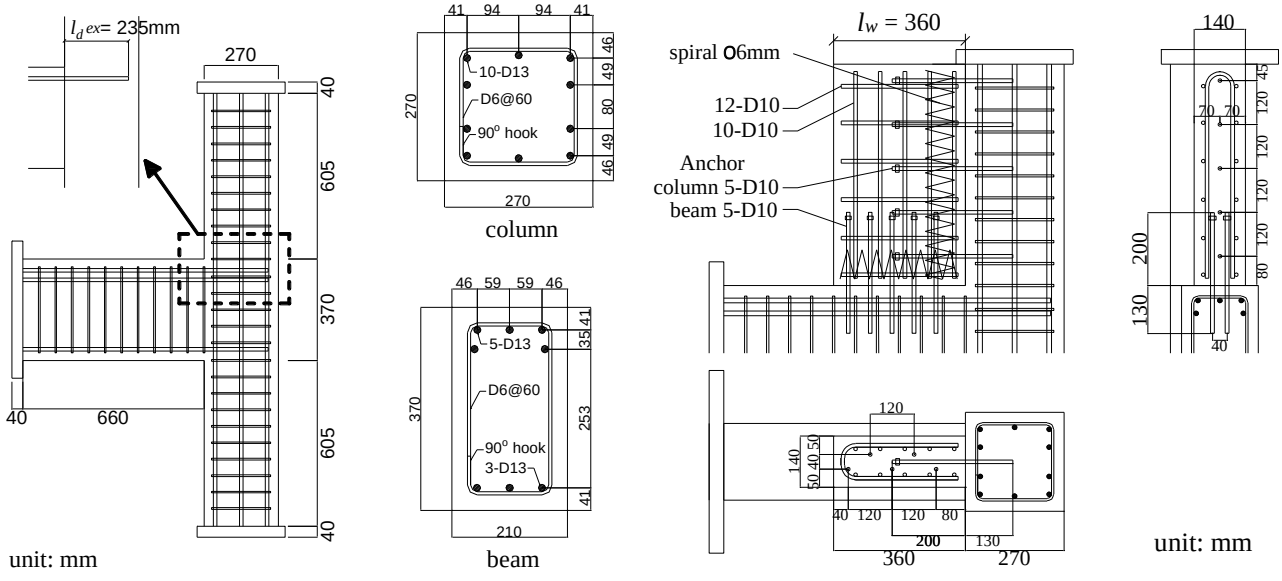

Fig. 2 – Details of specimen: (a) benchmark specimen, J1; (b) strengthened specimen, J1-W [2]

2.2 Experimental results

The applied joint moment and the drift ratio relationships of benchmark specimen, J1 and strengthened specimen, J1-W are shown in Fig. 3.

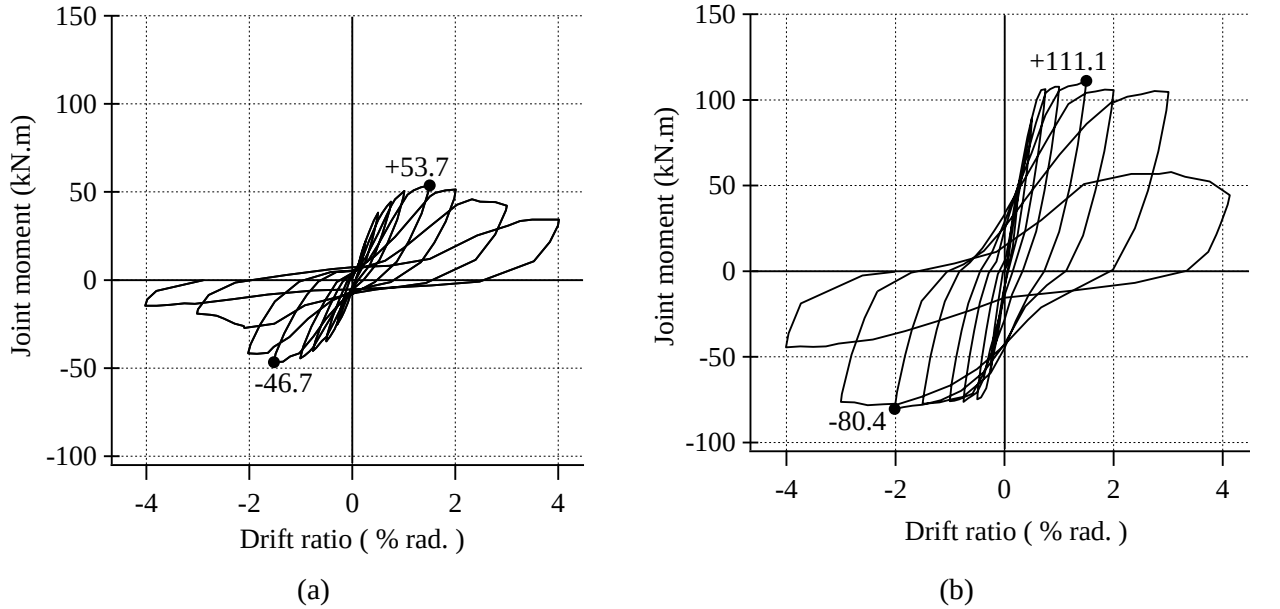

Fig. 3 – Joint moment vs. drift ratio relationships: (a) Specimen, J1; (b) Specimen, J1-W [2]

The benchmark specimen, J1, reached the maximum joint moments of 53.7 kN.m and 46.7 kN.m in the positive and negative direction, respectively. Substantial strength degradation was observed in the negative loading direction after attaining the peak load, as shown in Fig. 3(a). On the other hand, the strengthened specimen reached the maximums of 111.1 kN.m in the positive direction and 80.4 kN.m in the negative direction. The strength of J1-W was improved by 2.1 and 1.7 times compared to J1 in the positive and negative loading directions, respectively.

2.3 Failure process

In the benchmark specimen J1, diagonal cracks appeared at the joint region in ± 0.5% rad drift cycle. The bottom beam reinforcement at the column end yielded during the drift cycle of – 0.75% rad. Specimen reached the maximum strengths at ± 1.5% rad drift cycle followed by expansion on diagonal cracks to the upper column along the external longitudinal bars, indicating joint shear failure in the positive direction. While in the negative loading cycle, a wide vertical crack was observed on the beam-column joint face, as seen in Fig. 4, indicating anchorage failure of beam longitudinal reinforcement due to inadequate development length. In the subsequent negative loading cycle, a significant reduction in strength showed that anchorage failure was much more brittle in nature than the joint shear failure observed in the positive loading direction.

On the other hand, in the strengthened specimen J1-W, flexural shear cracks were observed at the beam ends attached to the wing walls in the ± 0.5% rad drift cycle. Diagonal cracks appeared in the beam-column joint panel during ± 0.75% rad drift cycle. During + 1.5% rad drift cycle, the maximum strength was observed. While for the negative direction, the maximum strength was observed in – 2% rad drift cycle. No significant strength reduction was observed up to ± 3% rad drift cycle. Subsequently, concrete crushing of beam was observed at the wing walls end, indicating shear failure of the beam. However, visible damage was not observed on the wing walls up to the last loading cycle of ± 4% rad. The strengthened specimen J1-W suffered severe damage at the beam end due to failure caused by a beam yielding mechanism, as seen in Fig. 5.

The deformation capacity of the specimen was evaluated as a point when the strength dropped to 80% of the maximum strength. The deformation capacity was improved by 155% in the negative direction through strengthening. From the experiment, it was seen that the failure mode of the structure was shifted from the brittle anchorage failure to the ductile beam flexural yielding failure. This showed that the deformation capacity of the structure was governed by the deformation capacity of the beam when strengthened by wing walls.

Fig. 4 – Damage to the specimen J1

Fig. 5 – Damage to the specimen J1-W

3. Evaluation of Beam Deformation Capacity

The ductility of the joint after strengthening was determined by the flexural-shear failure of the beam close to the wing walls end. This kind of failure might have occurred due to the reduction of shear span of the beam after the installation of wing walls. The evaluation concept of flexural-shear failure of the beam is shown in Fig. 6. This is important to prevent the failure of the building before reaching a minimum required deformation capacity.

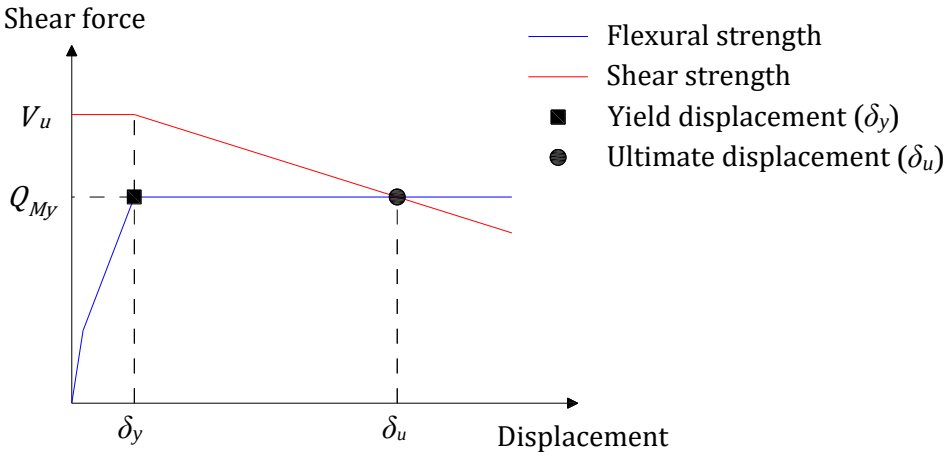

Fig. 6 – Conceptual drawing of evaluation of the deformation capacity of beams

3.1 Flexural performance curve

According to the design guidelines in Japan [4], the flexural performance curve of the beam was idealized by a trilinear function incorporating cracking point and yielding point, as shown in Fig. 7.

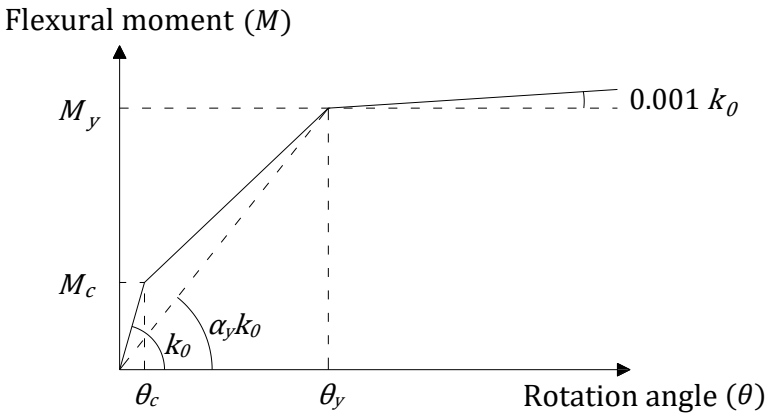

Fig. 7 – Trilinear moment-rotation relationship

Cracking moment M_c, yielding moment M_y and yielding rotation θ_y are given by Eqs. (3) to (7). The post-yield stiffness was assumed to be 0.001 of the elastic flexural stiffness (k_o).

$$M_c = 0.56\sqrt{f_c'}\ Z \tag{3}$$
$$M_y = 0.9\ a_t\ \sigma_y\ d \tag{4}$$
$$\theta_c = M_c\ /\ k_o \tag{5}$$
$$\theta_y = M_y\ /\ (\alpha_y\ k_o) \tag{6}$$
$$\alpha_y = \left(0.043 + 1.64\ \eta\ p_t + 0.043\ \frac{a}{d}\right)\left(\frac{d}{D}\right)^2 \tag{7}$$

where f_c' = compressive strength of concrete; Z = section modulus; a_t = area of tensile longitudinal reinforcement; σ_y = yield stress of longitudinal reinforcement; d = effective depth of beam; η = ratio of Young's modulus of reinforcement to that of concrete; p_t = tensile reinforcement ratio; a = shear span; D = total depth of beam.

3.2 Shear strength evaluation model

According to the Japanese design guidelines of AIJ 1997 [6], the shear strength of RC members was expressed as the minimum of Eqs. (8) to (10).

$$V_{u1} = \mu\ p_{we}\ \sigma_{wy}\ b_e\ j_e + \left(\nu\ \sigma_B - \frac{5\ p_{we}\ \sigma_{wy}}{\lambda}\right)\frac{b\ D}{2}\ tan\,\theta \tag{8}$$
$$V_{u2} = \frac{\lambda\ \nu\ \sigma_B + p_{we}\ \sigma_{wy}}{3}\ b_e\ j_e \tag{9}$$
$$V_{u3} = \frac{\lambda\ \nu\ \sigma_B}{2}\ b_e\ j_e \tag{10}$$

where μ = coefficient concerning the angle of concrete truss action; μ = 2–20R_p ; p_{we} = effective shear reinforcement ratio; $p_{we} = a_w/(b_e\ s)$; a_w = cross-sectional area of the shear reinforcement; b_e = effective width of the member; s = spacing of the shear reinforcement; σ_{wy} = yield stress of the shear reinforcement; j_e = effective depth of the member; $\nu = (1 - 20R_p)\nu_0$; $\nu_0 = 0.7 - \sigma_B/200$; λ = effective depth coefficient for truss action; $\lambda = 1 - s/2j_e - b_s/4j_e$; b_s = largest distance between ties; θ = angle of compression strut of arch mechanism; $tan\,\theta = 0.9\ \frac{D}{2L}$ when $\frac{L}{D} \geq 1.5$; $tan\,\theta = \frac{\sqrt{L^2+D^2}-L}{D}$ when $\frac{L}{D} < 1.5$; and L = clear length of the member.

Inter story-drift angle (θ) was determined as the ratio of column relative displacement (δ_h) to the column height (L_c), shown in Fig. 8. Beam displacement (δ) needs to be defined to evaluate the deformation capacity of the beam. Assuming that the column and the portion of the beam along the length of the wing walls are

rigid, considering minor damage to the column and wing walls, the drift angle (θ) is equal to the ratio of beam displacement (δ) to the free length of the beam (L_b-L_w).

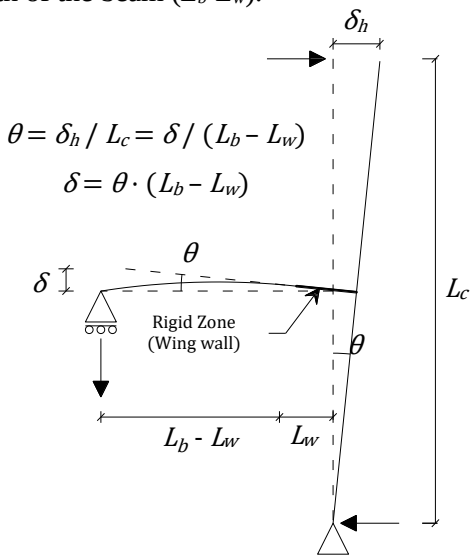

Fig. 8 – Converting drift angle to beam (with wing walls) displacement

The joint moment vs. drift ratio relationship of strengthened specimen J1-W of Fig. 3(b) was converted into the beam shear force vs. displacement relationship, as shown in Fig. 9. The figure also shows an estimation of the ultimate displacement based on the above models, which is approximately consistent with the experimental one. In the positive loading direction, the analytically computed deformation was 16mm, whereas the experimentally determined deformation was 20mm. On the other hand, in the negative loading direction, the analytically computed value and the experimentally determined value were 22mm and 21mm, respectively. These models are recommended for application to estimate the deformation capacity of the beam. Also, these results show that shear strengthening of the beam should be applied if a larger deformation capacity is expected in design.

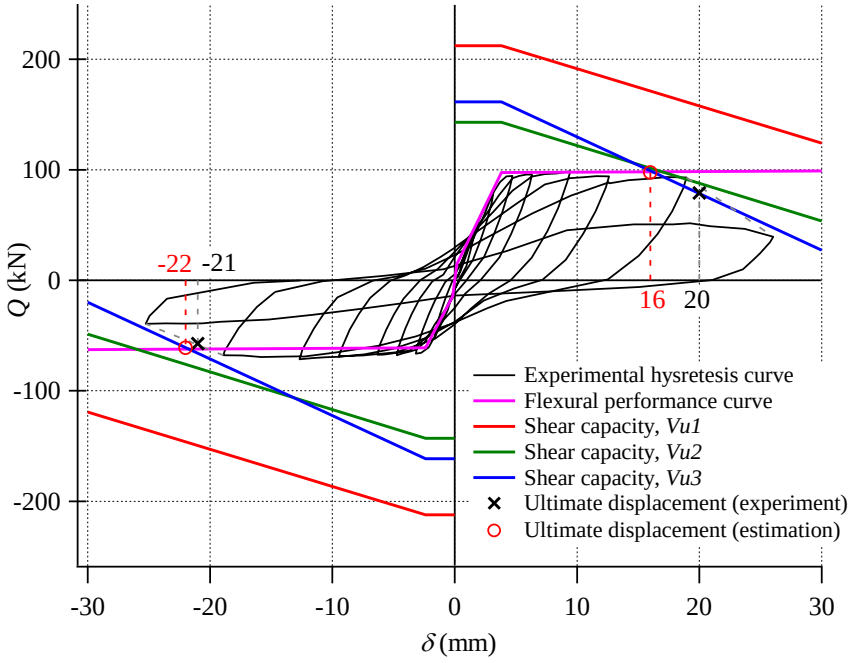

Fig. 9 – Estimated deformation capacity of the beam compared with the experimental results

4. Analytical Evaluation on the Seismic Performance of the Building of Interest

The previous section showed that the proposed method for strengthening the exterior beam-column joint with deficient anchorage by installing RC wing walls on the interior side of the column was effective. Furthermore, it is expected that this strengthening method will increase the global seismic performance of the building. Therefore, a series of static nonlinear pushover analyses were performed to evaluate the strength and deformation capacity of the building of interest under static lateral loads with and without installing wing walls on the exterior joints.

4.1 Analytical building

The strengthening by installing wing walls was applied to the building of interest focused on the previous experimental study. The strengthening with wing walls was considered on the interior side of the exterior columns for all stories of the building. Similar material properties as the experimental study were used for the analytical evaluation. The design strength of concrete was considered as f_c'= 10 MPa and the nominal strength of rebar was considered as f_y = 295 MPa for the existing building. However, for wing walls, design strength of concrete was considered as f_c' = 30 MPa.

4.2 Analytical assumptions

Pushover analysis was conducted for two models: the frame without wing walls and the frame with wing walls. The beams and columns were replaced by line elements with rigid zones at beam-column joints. Elastic springs

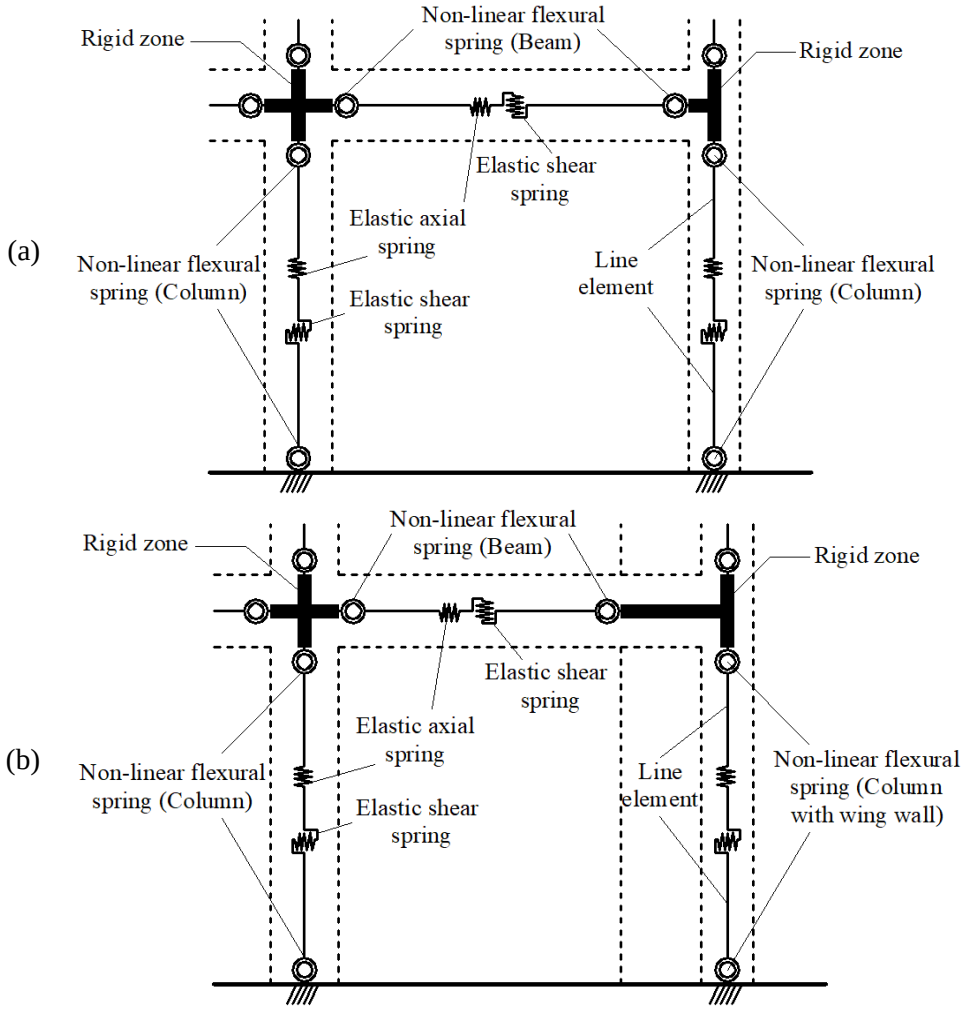

Fig. 10 – Modeling of the structural components: (a) Without wing walls (b) With wing walls

were considered in both axial and shear directions. Non-linear flexural spring was considered at the transition between the rigid and elastic zones. Figure 10 shows the general modeling of the members.

The flexural performance curve of the column was characterized by a trilinear function with cracking point and yielding point, as shown in Fig. 7, as per Japanese guidelines [4]. However, different equations were used for computing cracking moment and yielding moment of the column, as shown in Eqs. (11) to (13) considering axial load.

$$M_c = 0.56\sqrt{f_c'}\ Z + \frac{N\,D}{6} \tag{11}$$

$$M_y = 0.8\,a_t\,\sigma_y\,D + 0.5\,N\,D\left(1 - \frac{N}{b\,D\,f_c'}\right) \quad \text{for} \quad 0 < N \le 0.4\,b\,D\,f_c' \tag{12}$$

$$M_y = \left\{0.8\,a_t\,\sigma_y\,D + 0.12\,b\,D^2\,f_c'\right\}\left(\frac{N_{max} - N}{N_{max} - 0.4\,b\,D\,f_c'}\right) \quad \text{for} \quad 0.4\,b\,D\,f_c' < N \le N_{max} \tag{13}$$

where N = axial load on column; $N_{max} = b\,D\,f_c' + a_g\,\sigma_y$; a_g = total cross-sectional area of reinforcement.

In the case of column with wing walls, nonlinear flexural characteristics, elastic shear, and elastic axial deformation were considered. The flexural performance curve of the column with wing walls was characterized by a trilinear function similar to those of beam and column, as shown in Fig. 7. However, the following Eq. (14) was used for computing the cracking moment M_c [4]. The yielding moment M_y was calculated as the fully plastic moment by conventional bending analysis for the critical sections of the upper and lower columns with wing walls based on Navier's hypothesis [3]. It was assumed that all bars yielded on the tensile side and that concrete reached the ultimate strength; however, the bars on the compressive side were not considered [7].

$$M_c = \left(0.56\sqrt{f_c'} + \frac{N}{A}\right) Z + N \cdot e \tag{14}$$

$$M_{tension} = \sum a_{ti}\sigma_{yi}\left(d_i - \frac{\beta_1 x_n}{2}\right) + N\left(\frac{D_c}{2} - \frac{\beta_1 x_n}{2}\right) \tag{15}$$

$$M_{compression} = \sum a_{ti}\sigma_{yi}\left(d_i - \frac{\beta_1 x_n}{2}\right) + N\left(\frac{D_c}{2} + l_w - \frac{\beta_1 x_n}{2}\right) \tag{16}$$

where a_{ti}, σ_{yi}, and d_i are the area, yield stress and distance to the concrete compressive edge of the i-th tensile bar, respectively; β_1 = 0.85 for $f_c' \le 28$ MPa; β_1 = 0.85-0.007(f_c'-28) $\ge$ 0.65 for $f_c' > 28$ MPa; and x_n = depth of neutral axis, given by Eq. (17). This is based on the stress block concept according to ACI [7]; D_c = depth of column; l_w = length of wing wall.

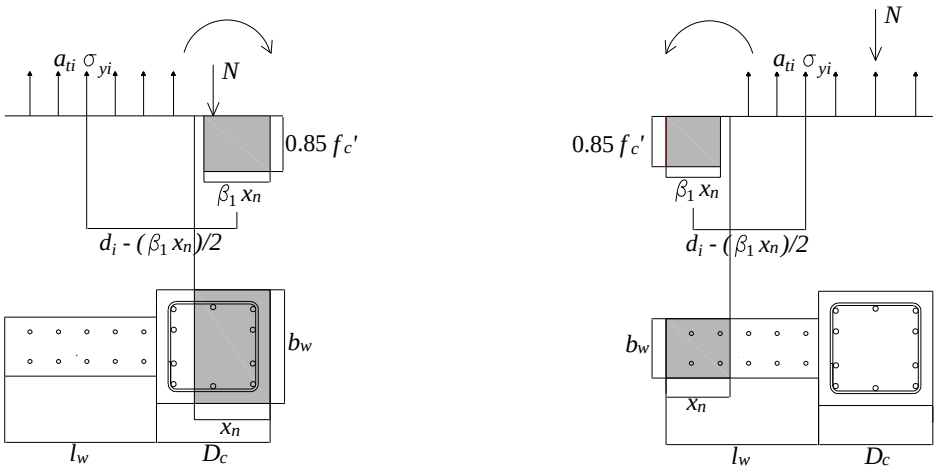

Fig. 11 – Ultimate strength for the column with wing walls: (a) tension (b) compression [2]

$$x_n = \frac{\sum a_{ti}\sigma_{yi} + N}{0.85\,\beta_1\,f_c'\,b_w} \tag{17}$$

where b_w = width of the stress block. The yielding rotation θ_y is assumed to be a constant value of 0.67%, based on the Japanese standard [4].

In the modeling, the foundations and slabs of the subject building were considered as rigid members. The gravity loads were calculated according to the Bangladesh National Building Code (BNBC) [1] and distributed to each node according to the tributary area. Lateral loads were determined according to BNBC [1] and an inverted triangular distribution was used for the distribution of lateral forces.

4.3 Analysis results

Only the negative direction was considered in pushover analysis because the frame without wing walls was expected to fail by anchorage failure, as explained in Section 2. The base shear force vs. the drift angle at roof level is shown in Fig. 12.

The performance limit for the case of the frame without wing walls was taken as the point in which the start of strength degradation was observed during the experiment. Benchmark specimen, J1, reached the maximum strength in the negative loading direction at a drift ratio of 1.5% rad, shortly followed by degradation of strength due to the failure of the joint. Therefore, the performance limit of the frame was set to the point when the rotation of the beam end at an exterior joint reached a drift angle of 1.5% rad. The performance limit of the frame was obtained at a roof-drift angle of 0.87% and the corresponding base shear force was 1030 kN.

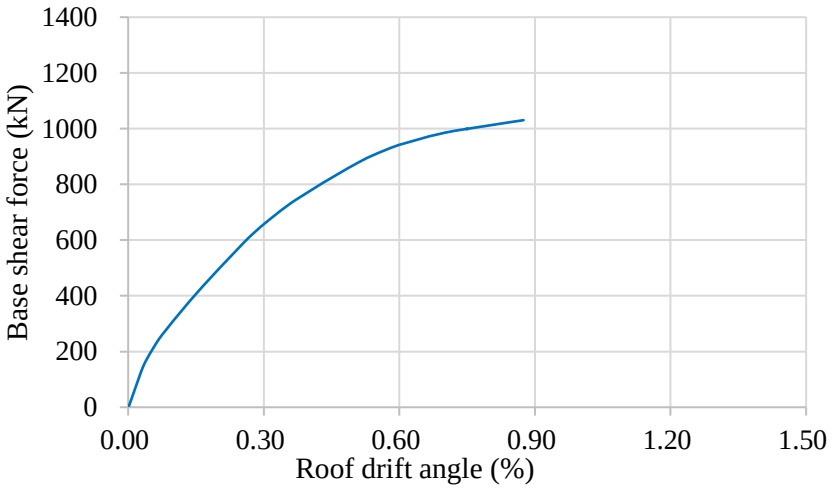

Fig. 12 – Base shear force vs. roof drift relationship for the frame without wing walls

On the other hand, for the frame with wing walls, the performance limit was controlled by the flexural-shear failure of the beam since the beam span was shortened after the installation of wing walls. The shear capacity of the beam was calculated by the AIJ 1997 shear strength model [6], as shown in Section 3.2. The beam shear force (Q) was calculated by Eq. (18), and the total deformation of the beam (δ) was calculated by Eq. (19). Figure 13 shows the evaluation results of the deformation capacity of the beam connected to the exterior joint with wing walls. The ultimate displacement of the beam in the frame with wing walls was estimated to be 61 mm, equal to a beam drift angle of 2.95% rad. If a larger deformation capacity is expected in the design of the strengthened building, shear strengthening of the beam needs to be applied.

$$Q = \frac{M_A + M_B}{L} \tag{18}$$

$$\delta = \delta_f + \delta_s \tag{19}$$

where, M_A , M_B = moment at both ends of the beam, obtained from flexural spring; L = clear span of the beam; δ_f = flexural deformation, obtained from the rotation (θ) of the flexural spring, assuming a fixed point of

contra flexure at the mid-span of the beam, as shown in Fig. 14; and δ_s = shear deformation, obtained as deformation of the shear spring from the pushover analysis.

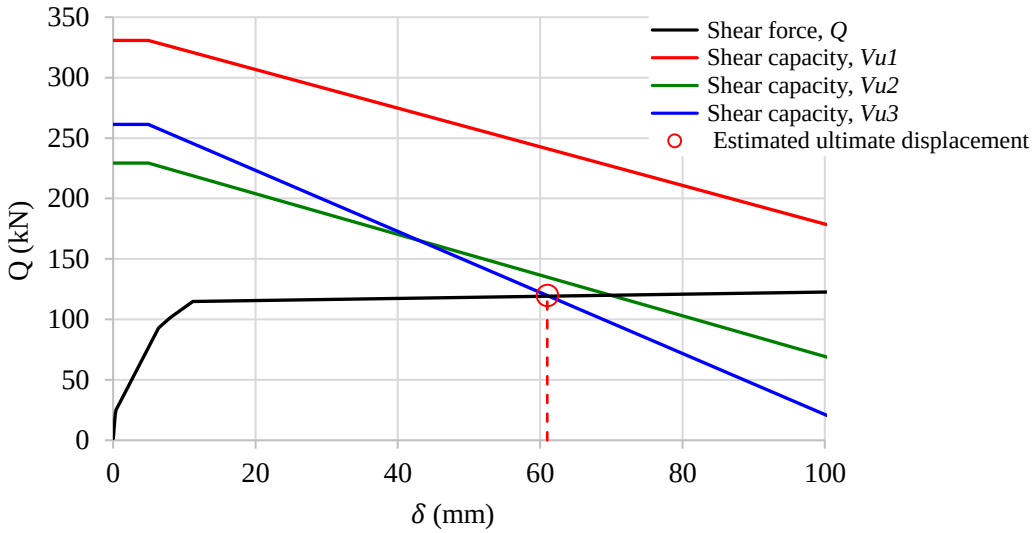

Fig. 13 – Estimated deformation capacity of the beams

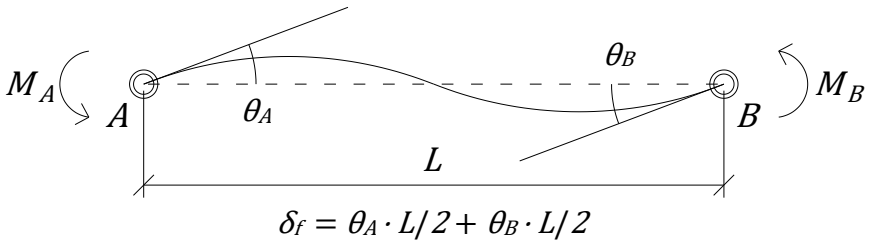

Fig. 14 – Flexural deformation from the flexural spring

The base shear force vs. drift angle relationship at the roof level for the frame strengthened with wing walls is shown in Fig. 15. The performance limit of the frame with wing walls was obtained at a roof drift angle of 1.32% and the corresponding base shear force was 1278 kN.

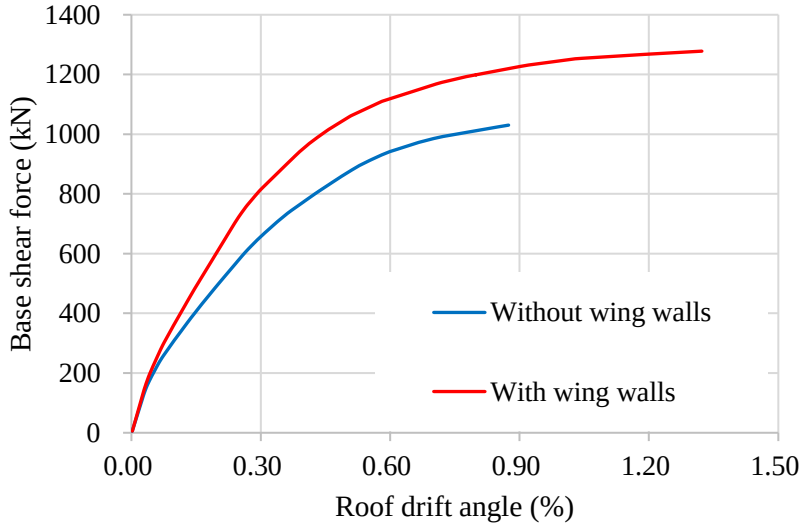

Fig. 15 – Base shear force vs. roof drift relationships for the frames with and without wing walls

From the evaluation results, it can be seen that both lateral strength and deformation capacity of the building was improved after strengthening with wing walls. The lateral strength of the strengthened building increased by 24% and deformation capacity was improved by 52% compared to the building without strengthening.

5. Conclusions

The experimental results showed that the proposed design concept considering the length of the wing walls to extend the development length was adequate to prevent the brittle anchorage failure. After the installation of wing walls, the structural deformation capacity was governed by the beam deformation limit due to the reduction of beam span length. The preceding process can be used to determine the performance limit of building with wing walls where the flexural-shear failure of the beam is governed. From the analytical results, it can be seen that the installation of wing walls improves the global seismic performance of buildings with deficient beam rebar anchorage in terms of both the strength and the deformation capacity of the building.

6. Acknowledgments

This research was supported by the SATREPS project under JICA/JST supervision headed by Prof. Yoshiaki Nakano, The University of Tokyo. The authors would like to show their gratitude to them.

7. References

[1] Housing and Building Research Institute, “Bangladesh National Building Code (BNBC) 2015 Final Draft,” 2015.

[2] Wardi S, Sanada Y, Saha N, Takahashi S, “Improving integrity of RC beam-column joints with deficient beam rebar anchorage”, *Earthquake Engng Struct Dyn.*, 2020, 1-27, https://doi.org/10.1002/eqe.3229

[3] Li Y and Sanada Y, “Seismic strengthening of existing RC beam-column joints by wing walls,” *Earthquake Engng Struct. Dyn.*, vol. 41, no. 11, pp. 1549–1568, 2017.

[4] Architectural Institute of Japan (AIJ), “AIJ Standard for Structural Calculation of Reinforced Concrete Structures revised 2018 (in Japanese),” 2018.

[5] JBDPA (The Japan Building Disaster Prevention Association), “Standard for Seismic Evaluation of Existing Reinforced Concrete Buildings, 2001, Guidelines for Seismic Retrofit of Existing Reinforced Concrete Buildings, 2001 and Technical Manual for Seismic Evaluation and Seismic Retrofit of Existing Reinforced Concrete,” 2005.

[6] Architectural Institute of Japan (AIJ), “Design guideline for earthquake resistant reinforced concrete buildings based on inelastic displacement concept,” 1997.

[7] Li Y, Sanada Y, Takahashi S, Maekawa K, Choi H, and Matsukawa K, “Seismic Performance Evaluation and Strengthening of RC Frames with Substandard Beam-Column Joint: Lessons Learned from the 2013 Bohol Earthquake,” *J. Earthq. Tsunami*, vol. 10, no. 03, p. 1640007, 2016.

